Role of the histone domain in the autoinhibition and activation of the Ras activator Son of Sevenless

Jodi Gureasko[a,1], Olga Kuchment[a,1], Debora Lika Makino[a,3], Holger Sondermann[a,4], Dafna Bar-Sagi[b], and John Kuriyan[a,c,2]

[a]Department of Molecular and Cell Biology, Department of Chemistry, and Howard Hughes Medical Institute, QB3 Institute, 176 Stanley Hall, University of California, Berkeley, CA 94720; [b]Department of Biochemistry, New York University School of Medicine, New York, NY 10016; and [c]Physical Biosciences Division, Lawrence Berkeley National Laboratory, Berkeley, CA 94720

Contributed by John Kuriyan, December 5, 2009 (sent for review October 7, 2009)

Membrane-bound Ras is activated by translocation of the Son of Sevenless (SOS) protein to the plasma membrane. SOS is inactive unless Ras is bound to an allosteric site on SOS, and the Dbl homology (DH) and Pleckstrin homology (PH) domains of SOS (the DH-PH unit) block allosteric Ras binding. We showed previously that the activity of SOS at the membrane increases with the density of PIP_2 and the local concentration of Ras-GTP, which synergize to release the DH-PH unit. Here we present a new crystal structure of SOS that contains the N-terminal histone domain in addition to the DH-PH unit and the catalytic unit (SOS^{HDFC}, residues 1–1049). The structure reveals that the histone domain plays a dual role in occluding the allosteric site and in stabilizing the autoinhibitory conformation of the DH-PH unit. Additional insight is provided by kinetic analysis of the activation of membrane-bound Ras by mutant forms of SOS that contain mutations in the histone and the PH domains (E108K, C441Y, and E433K) that are associated with Noonan syndrome, a disease caused by hyperactive Ras signaling. Our results indicate that the histone domain and the DH-PH unit are conformationally coupled, and that the simultaneous engagement of the membrane by a PH domain PIP_2-binding interaction and electrostatic interactions between a conserved positively charged patch on the histone domain and the negatively charged membrane coincides with a productive reorientation of SOS at the membrane and increased accessibility of both Ras binding sites on SOS.

crystal structure | membrane-binding | PIP2-dependent | SOS

The activation of membrane-bound Ras, a central regulator of cell proliferation and differentiation, is associated with its conversion from the GDP- to the GTP-bound form. This process of nucleotide exchange is triggered by the growth factor-dependent membrane recruitment of the Ras-specific guanine nucleotide exchange factor Son of Sevenless (SOS) (1, 2). SOS has two binding sites for Ras, one of which is an allosteric site that is distal to the active site (3). Binding of Ras at this site stimulates the nucleotide exchange activity of SOS allosterically, by causing conformational changes at the active site that allow substrate Ras to bind (3, 4). The importance of the allosteric Ras binding site has been underscored by the finding that it is required for robust T-cell activation (5, 6) and for the sustained activation of Ras-ERK signaling (7).

The unchecked activation of Ras by SOS is prevented by the N-terminal regulatory segment that contains a domain with two histone-like folds (the histone domain), followed by Dbl-homology (DH) and pleckstrin-homology (PH) domains (the DH-PH unit). The DH domain occludes the allosteric site (8), and thereby blocks the localization of SOS to the membrane by allosteric Ras (9). The PH domain is closely associated with the DH domain (10) and binds to phosphatidylinositol-4,5-bisphosphate (PIP_2) (11–14) and to phosphatidic acid (PA) (15).

The histone domain (residues 1–191; see Fig. 1*A*) has significant sequence similarity to nucleosomal histones and its structure resembles that of a histone dimer (16–18). This is surprising because SOS is neither localized to the nucleus nor involved in DNA or RNA binding, as is the case for other proteins with histone-like folds. It has been speculated that the histone domain of SOS might retain a distant functional connection to the recognition of nucleotide phosphate groups by histone domains in nucleosomes (19). The histone domain interacts with the rest of SOS using a patch of highly conserved residues that in nucleosomes are involved in the formation of histone tetramers. Computational modeling suggests that the histone domain might interact with phospholipid headgroups in the membrane by using a conserved region of positive electrostatic potential that corresponds to the DNA-binding surface of nucleosomes, implicating the histone domain in mediating membrane-dependent activation signals (19).

We have shown recently, by studying the kinetics of nucleotide exchange by SOS when Ras is tethered to phospholipid membranes, that the allosteric site can serve as a membrane-docking site for SOS through interaction with Ras, thereby tethering SOS to the membrane and consequently increasing the chance of productive Ras-SOS encounters (9). PIP_2 binding to the PH domain releases autoinhibition by the DH-PH unit. At the membrane, high concentrations of PIP_2 and Ras-GTP can function cooperatively to potentiate Ras activation by SOS (9). The PH domain has also been shown to mediate SOS membrane targeting through binding to PA (15).

The histone domain confers an additional level of autoinhibitory regulation to SOS. Some patients with Noonan syndrome, a developmental disorder characterized by learning problems and congenital heart defects (20), have a gain-of-function SOS1 mutation in the helical PH-Rem linker (R552G) that connects the N-terminal regulatory segment to the catalytic unit (SOS^{cat}) (Fig. 1). Mutation of R552G in the PH-Rem linker disrupts the internal docking of the histone domain onto the rest of SOS (19). Deletion of the histone domain or the presence of the Noonan syndrome-associated mutation, R552G (21, 22), increases SOS activity in a PIP_2-dependent manner (9). Interestingly, the histone domain does not interfere with the binding of SOS to PIP_2-containing vesicles (9). These results do not, therefore, explain how the histone domain impedes SOS activation, nor do they explain how the inhibition of the histone domain is alleviated during the activation of SOS.

In this paper we present a new crystal structure of SOS at 3.2 Å resolution that contains the histone domain and the DH-PH unit

Author contributions: J.G., O.K., and J.K. designed research; J.G. and O.K. performed research; J.G., O.K., and D.L.M. contributed new reagents/analytic tools; J.G., O.K., D.L.M., H.S., D.B.-S., and J.K. analyzed data; J.G. and J.K. wrote the paper.

The authors declare no conflict of interest.

Freely available online through the PNAS open access option.

[1]These authors contributed equally to this work.

[2]To whom correspondence should be addressed. E-mail: kuriyan@berkeley.edu.

[3]Present address: Department of Structural Cell Biology, Max Planck Institute of Biochemistry, Am Klopferspitz 18, D-82152 Martinsried, Germany

[4]Present address: Department of Molecular Medicine, College of Veterinary Medicine, Cornell University, Ithaca, NY 14853

This article contains supporting information online at www.pnas.org/cgi/content/full/0913915107/DCSupplemental.

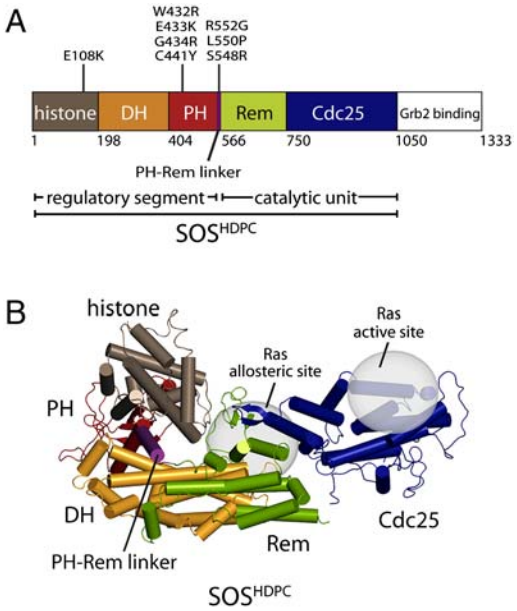

Fig. 1. Structure of SOS^{HDPC}. (*A*) Domain organization of SOS, with the Noonan syndrome-associated mutations that map to the histone domain, the PH domain and the PH-Rem linker indicated. (*B*) Crystal structure of SOS^{HDPC}, with coloring according to the diagram in (*A*).

in addition to the catalytic segment (SOS^{HDPC}, residues 1–1049). This construct lacks only the C-terminal segment (residues 1050–1333) that contains the binding sites for the adaptor protein Grb2 (23–26). The structure of autoinhibited SOS^{HDPC} reveals that the histone domain has the dual role of directly participating in the occlusion of the allosteric site and in stabilizing the inhibitory conformation of the DH-PH unit. Additional insight is provided by investigation of the Noonan syndrome-associated mutations in SOS that map to the histone and PH domains (E108K, C441Y, and E433K) (21, 22), and are found to activate SOS only in a membrane context and in the presence of PIP_2. Our data indicate that the histone domain and the DH-PH unit are conformationally coupled, and that in the presence of sufficiently strong input signals, the histone domain and the DH-PH unit synergize to increase the efficiency of SOS membrane-binding and activation of SOS on membranes.

Results and Discussion

Crystal Structure of SOS^{HDPC}. We determined the crystal structure of autoinhibited SOS^{HDPC} (residues 1–1049) at 3.2 Å resolution (Fig. 1*B* and Table S1). The structure was solved by molecular replacement using separate search models for the histone (18), DH (10), Rem, and Cdc25 domains (8). Despite the moderate resolution of the analysis we found it necessary to refine individual atomic positions because of localized changes with respect to the molecular replacement models in certain loop regions. The PH domain is relatively poorly ordered in these crystals and so we treated the PH domain as a single rigid body, using its structure as defined in SOS^{DPC} (8). The current model has been refined to an R value of 26.0% and a free R value of 31.2% (Table S1). The five N-terminal residues and residues in the linker between the histone and DH domains (178–194), the linker between the DH and PH domains (405–417), the linker between the Rem and Cdc25 domains (747–749) and the four C-terminal residues are disordered and are not included in the final model.

An approximate model for how the histone domain docks onto the rest of SOS was obtained previously by small angle x-ray scattering and computational docking (19). The crystal structure of SOS^{HDPC} confirms that the earlier model was correct in a general sense, but there are substantial differences in the details of the interdomain interfaces and the orientation of the histone domain with respect to the rest of SOS. As predicted previously (19), the histone domain binds to the rest of SOS by packing against the helical PH-Rem linker that connects the N-terminal regulatory segment to the catalytic unit (SOS^{cat}) (Fig. 1). The location of the histone domain is such that it wedges between the DH, PH, and Rem domains, where it interacts most extensively with the DH domain and the PH-Rem linker while making glancing contacts with the PH and Rem domains (Fig. 1*B*).

The Histone Domain Occludes the Allosteric Site and Stabilizes the DH-PH Unit in the Inhibitory Conformation. We had suggested previously that the histone domain might constrain SOS activation by preventing the simultaneous engagement of the membrane by the PH domain and the two Ras binding sites of SOS (9). The structure of SOS^{HDPC} reveals that the histone domain also impedes the activity of SOS by directly occluding the allosteric Ras binding site (Fig. 2).

A conserved network of interactions formed by the histone domain, the DH domain and the PH-Rem linker appears to stabilize SOS in the autoinhibited conformation (Fig. 3*A*). As shown earlier (19), a critical interaction in the interface between the histone domain and the PH-Rem linker is the formation of ion pairing interactions between R552 in the PH-Rem linker and D140 and D169 in the histone domain (Fig. 3*A*). D169 also forms a hydrogen bond with S548 in the PH-Rem linker (Fig. 3*A*). Each of these residues is invariant across SOS sequences (see Fig. S1 for a sequence alignment of SOS proteins). Mutation of R552 or D140 completely abolishes the noncovalent interaction of the histone domain with the rest of SOS (19). The importance of this interface in the autoinhibitory regulation of SOS is highlighted by the Noonan syndrome-associated mutations, R552G and S548R (21, 22), both of which increase the activity of SOS proteins when Ras is coupled to membranes containing PIP_2 (9) (see Fig. 3*B*).

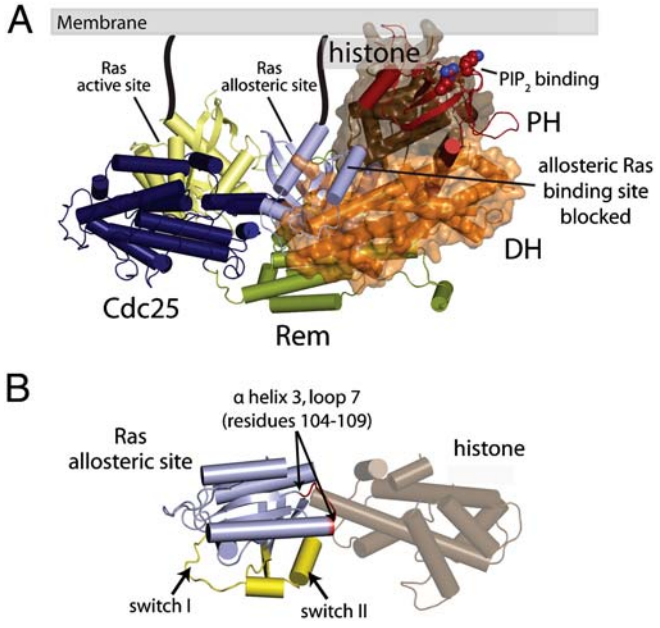

Fig. 2. Allosteric Ras binding site is occluded by the histone and the DH domains. (*A*) The structure of autoinhibited SOS^{HDPC} is shown at the membrane. To model Ras at both the active and allosteric Ras binding sites, the structures of SOS^{HDPC} and the ternary Ras:SOS^{cat}:Ras-GTP complex (3) were aligned through superpositioning of the two respective Rem domains of SOS^{HDPC} and SOS^{cat}. Note that the Ras-GTP bound at the allosteric site in the ternary complex overlaps with the histone and the DH domains of SOS^{HDPC}. (*B*) Close up view of the occlusion of the allosteric site by the histone domain. Only the histone domain from SOS^{HDPC} and the Ras-GTP from the ternary complex are shown for clarity.

BIOCHEMISTRY

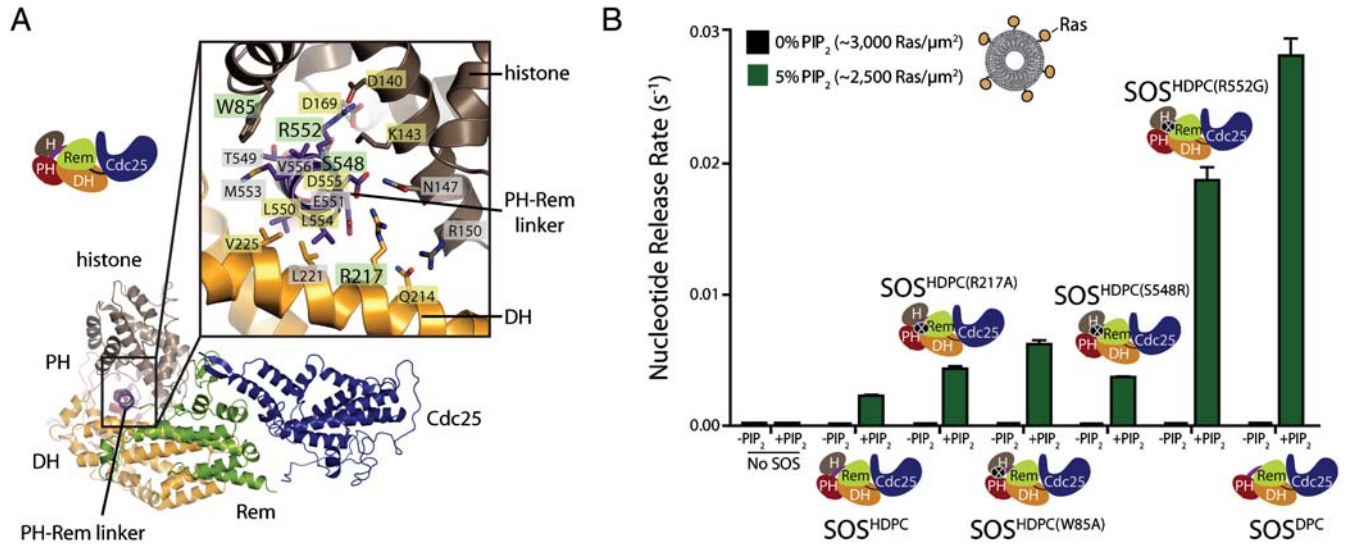

Fig. 3. Kinetic analysis of SOS constructs containing mutations in the inhibitory histone domain interface. (*A*) Detailed view showing the conserved network of interactions between the histone domain, the DH domain, and the PH-Rem linker. Amino acid residues mutated and analyzed in (*B*) are shown in green, and additional highly conserved residues are indicated in yellow. (*B*) Nucleotide exchange rates for $SOS^{HDPC(W85A)}$, $SOS^{HDPC(R217A)}$, $SOS^{HDPC(S548R)}$, $SOS^{HDPC(R552G)}$, SOS^{HPDC}, and SOS^{DPC} in the absence and presence of PIP_2 in Ras-coupled vesicles are compared (mant-dGDP is exchanged for unlabeled GTP; bulk concentration of Ras and SOS is 1 μM and 100 nM, respectively). $SOS^{HDPC(R217A)}$ and $SOS^{HDPC(W85A)}$ contain mutations that weaken the histone-DH domain interface and the interface between the histone domain and the PH-Rem linker, respectively. $SOS^{HDPC(S548R)}$ and $SOS^{HDPC(R552G)}$ contain amino acid substitutions in the PH-Rem linker that cause Noonan syndrome (21, 22). Note that in contrast to SOS^{HDPC}, the activity of $SOS^{HDPC(W85A)}$, $SOS^{HDPC(R217A)}$, $SOS^{HDPC(S548R)}$, and $SOS^{HDPC(R552G)}$ is increased in a PIP_2-dependent manner.

The histone domain is positioned so as to reinforce the position of the PH-Rem linker and the inhibitory DH domain. K143, N147, and R150 in the histone domain interact with the conserved Q214 and invariant R217 in the DH domain and the invariant D555 in the PH-Rem linker (Fig. 3*A*). Two surrounding hydrophobic clusters further stabilize these ionic interactions. L550 and L554 (both invariant) in the PH-Rem linker pack against a conserved hydrophobic patch on the DH domain, and W85 in the histone domain packs against a conserved hydrophobic patch on the PH-Rem linker (Fig. 3*A*). Together, these interactions anchor the PH-Rem linker at each end and fix the position of the inhibitory histone and DH domains.

To assess the functional significance of these interactions in the regulation of SOS activity, we replaced R217 and W85 by alanine (Fig. 3*A*). The activities of six SOS constructs, five with the histone domain ($SOS^{HDPC(W85A)}$, $SOS^{HDPC(R217A)}$, $SOS^{HDPC(R552G)}$, $SOS^{HDPC(S548R)}$, and SOS^{HPDC}) and one without (SOS^{DPC}), were compared in the absence and presence of PIP_2 in Ras-coupled vesicles (Fig. 3*B*). As seen previously for wild-type SOS (9), in the absence of PIP_2 all of the SOS constructs ($SOS^{HDPC(W85A)}$, $SOS^{HDPC(R217A)}$, $SOS^{HDPC(S548R)}$, $SOS^{HDPC(R552G)}$, SOS^{HPDC}, and SOS^{DPC}) have very low levels of activity, with kinetics essentially indistinguishable from unstimulated nucleotide release from Ras (Fig. 3*B*). In contrast to SOS^{HDPC}, inclusion of PIP_2 in membranes results in partial activation of $SOS^{HDPC(W85A)}$, $SOS^{HDPC(R217A)}$, and the Noonan syndrome-associated mutations, $SOS^{HDPC(S548R)}$ and $SOS^{HDPC(R552G)}$, and a marked increase in the activity of SOS^{DPC} (Fig. 3*B*). These results demonstrate that W85, R217, S548, and R552 are important components of the inhibitory histone domain interface, consistent with the earlier finding that the docking of the histone domain is crucial for inhibition (9). Our results, therefore, indicate that the regulation of SOS by the histone domain involves a strengthening of the autoinhibitory interactions between the histone domain and the rest of SOS. Mutations that destabilize the inhibitory histone domain interface sensitize SOS to PIP_2 and allosteric Ras, and thus promote the PIP_2-dependent release of the DH-PH unit, opening the allosteric site.

Membrane-dependent electrostatic switch releases the inhibition by the histone domain. A highly conserved positively charged surface of the histone domain was predicted to be a potential membrane

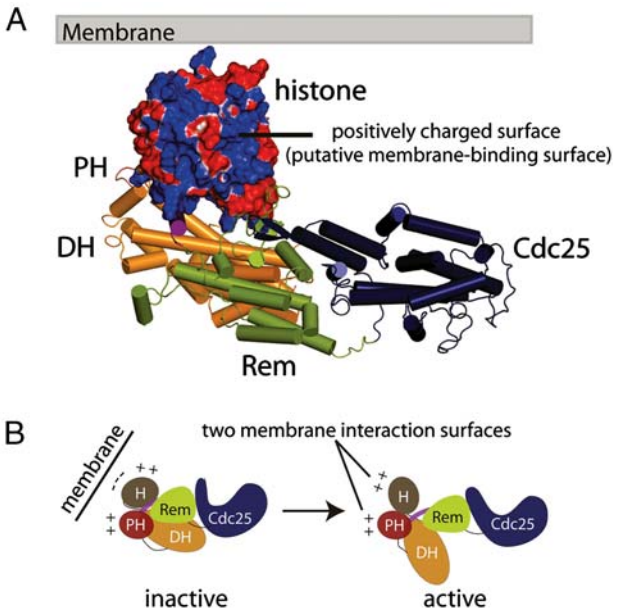

Fig. 4. A membrane-dependent electrostatic switch releases the histone domain. (*A*) The electrostatic surface potential of the histone domain of autoinhibited SOS^{HDPC} is shown at the membrane, with positive and negative surface potentials colored blue and red, respectively. Electrostatic surface calculations were performed using the APBS Tools plugin for PyMOL (38). SOS is oriented so that both Ras-binding sites are positioned appropriately for connection to the membrane, while also positioning the lipid-interacting face of the PH domain toward the membrane. Note that in the autoinhibited conformation, the negatively charged surface of the histone domain is oriented toward the membrane, whereas the putative membrane-binding surface (19) is oriented roughly orthogonal to it. (*B*) The simultaneous engagement of the membrane by the histone and the PH domains coincides with a productive reorientation of SOS in the plane of the membrane.

interaction surface (19). To see how the histone domain might interact with the membrane we aligned SOS so that both Ras binding sites are roughly in a plane parallel to the membrane, while also positioning the lipid-interacting face of the PH domain toward the membrane. When the structure of autoinhibited SOS^{HDPC} is oriented in this way it is apparent that the positively charged surface of the histone domain does not face in the direction of the membrane, and is instead oriented roughly orthogonal to it (Fig. 4*A*). This orientation places a negatively charged surface of the histone domain facing toward the membrane (Fig. 4*A*).

We speculate that the large conformational rearrangement of the histone and the DH domains that is required for SOS activation might correspond to a reconfiguration of the histone domain, such that its positively charged surface interacts with the negatively charged membrane (Fig. 4*B*). Such a conformational rearrangement could facilitate SOS activation by disrupting the inhibitory interactions between the histone domain and the rest of SOS and by providing an additional membrane-anchorage point for SOS, thereby increasing the efficiency with which membrane-bound Ras-GTP is able to access the SOS allosteric site.

To test this hypothesis, we made use of a Noonan syndrome-associated variant of SOS in which E108 is replaced by lysine (E108K) (21, 22). E108 resides in the center of the positively charged region on the surface of the histone domain, and its replacement by lysine increases the net positive charge of the postulated membrane interaction surface (Fig. 5*A*). We wondered whether this mutation might potentiate SOS activity by strengthening the interaction of the histone domain with the membrane, thereby triggering the necessary conformational change.

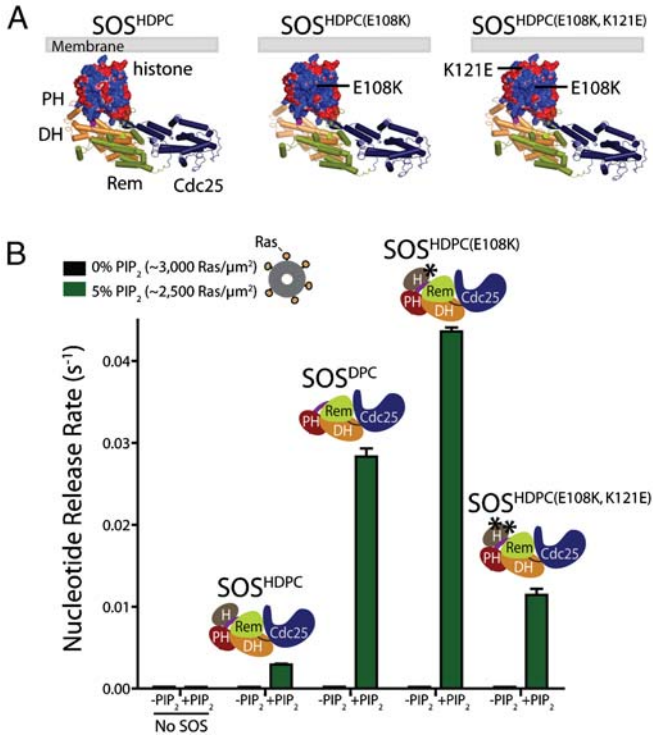

Fig. 5. Synergy between the histone domain and the DH-PH unit is crucial for effective membrane-binding and activation of SOS on membranes. (*A*) The electrostatic surface potentials of SOS^{HDPC} and constructs of SOS^{HDPC} containing the Noonan syndrome-associated mutation (E108K) in the absence and presence of K121E are compared. Electrostatic surface calculations were performed as described in the legend of Fig. 4. (*B*) Nucleotide exchange rates for SOS^{HDPC}, $SOS^{HDPC(E108K)}$, $SOS^{HDPC(E108K,K121E)}$, and SOS^{DPC} in the absence and presence of PIP_2 in Ras-coupled vesicles are compared (mant-dGDP is exchanged for unlabeled GTP; bulk concentration of Ras and SOS is 1 μM and 100 nM, respectively). Note the ability of the E108K mutation to greatly potentiate the PIP_2-dependent activation of $SOS^{HDPC(E108K)}$.

We performed experiments in which 100 nM SOS^{DPC}, SOS^{HDPC} and $SOS^{HDPC(E108K)}$ were used to stimulate nucleotide exchange from membrane-bound Ras (Fig. 5*B*). Inclusion of PIP_2 in Ras-coupled membranes results in a marked increase in the activity of SOS constructs containing the Noonan syndrome-associated mutation ($SOS^{HDPC(E108K)}$) or in which the histone domain is entirely deleted (SOS^{DPC}) (Fig. 5*B*). Moreover, the PIP_2-dependent activity of $SOS^{HDPC(E108K)}$ is greater than that observed for SOS^{DPC} (Fig. 5*B*). This suggests that the histone domain might play an important role in regulating SOS membrane-association and activity. Consistent with this idea is the observation that, in addition to increasing the localization of the histone domain of SOS to the plasma membrane in cells, the presence of the Noonan syndrome-associated mutation, E108K, in SOS leads to an increase in the basal level of active Ras and prolonged Ras activation after EGF stimulation (27).

We also tested the activity of a construct of SOS containing a substitution of K121 by glutamate (K121E) in addition to the Noonan syndrome mutation, E108K ($SOS^{HDPC(E108K,K121E)}$). K121 is invariant in SOS from C. elegans to humans, and it lies on the ridge between the negatively charged and positively charged faces of the histone domain (Fig. 5*A*). Mutation of K121E in $SOS^{HDPC(E108K,K121E)}$ decreases the net positive charge on the putative membrane-binding surface of the histone domain, and should, therefore, decrease the apparent affinity of the positively charged surface of the histone domain for the negatively charged membrane. Fig. 5*B* compares the activities of four SOS constructs, three with the histone domain ($SOS^{HDPC(E108K)}$, $SOS^{HDPC(E108K,K121E)}$, and SOS^{HPDC}) and one without (SOS^{DPC}), in the absence and presence of PIP_2 in Ras-coupled vesicles. Mutation of K121E in $SOS^{HDPC(E108K,K121E)}$ leads to a reduction in the PIP_2-dependent activation of $SOS^{HDPC(E108K)}$ (Fig. 5*B*), further supporting a role for nonspecific electrostatic interactions of the histone domain with the membrane in release of autoinhibition and activation of SOS on membranes. Data in the accompanying paper (27) indicate that PA and PIP_2 bind to the histone domain at different sites, and that interactions of the histone domain with PA also results in similar activation. Our in vitro assays do not demonstrate an effect of PA on SOS activity, as noted previously (9). Resolution of this discrepancy awaits further experimentation.

Cooperative Release of the Histone Domain and the DH-PH Unit. PIP_2 binding to the PH domain could stimulate SOS activity by increasing the local concentration of SOS on membranes (9). Constructs of SOS containing mutations that weaken the DH-Rem interface, and thus stimulate SOS activity by facilitating access of Ras to the allosteric site (8), still require PIP_2 for full relief of the inhibitory effect of the DH domain (see Fig. S2). This raises the possibility that in addition to increasing the local concentration of SOS on membranes, the PH domain-PIP_2 binding interaction might play a role in allowing Ras to bind to the allosteric site on SOS more efficiently. Thus, it seems that synergy between the histone domain and the DH-PH unit is crucial for effective membrane-binding and release of autoinhibition. Further studies are required to delineate the extent to which the histone domain and the DH-PH unit are conformationally coupled, and to define how a membrane-dependent electrostatic switch in the configuration of the histone domain coincides with a productive reorientation of SOS in the plane of the membrane.

Four of the conserved amino acid residues in SOS that are altered by Noonan syndrome-associated mutations lie within the PH domain (W432R, E433K, G434R, and C441Y) (21, 22), in a region close to the very small interface involving only a few amino acids between the histone and the PH domains. To determine if the ability of these mutations to activate SOS

BIOCHEMISTRY

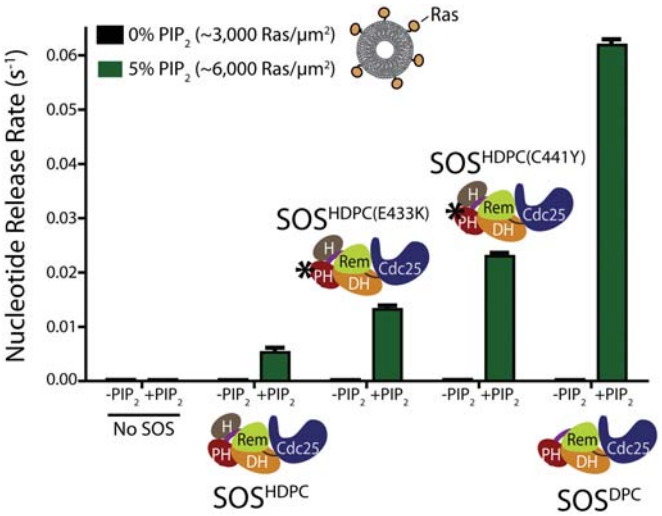

Fig. 6. PIP_2-dependent activation of the PH domain-associated Noonan syndrome mutations in SOS. Nucleotide exchange rates for SOS^{HDPC}, $SOS^{HDPC(E433K)}$, $SOS^{HDPC(C441Y)}$, and SOS^{DPC} in the absence and presence of PIP^2 in Ras-coupled vesicles are compared (mant-dGDP is exchanged for unlabeled GTP; bulk concentration of Ras and SOS is 1 μM and 100 nM, respectively). Note that the activity of the Noonan syndrome-associated mutations, $SOS^{HDPC(E433K)}$ and $SOS^{HDPC(C441Y)}$, is increased relative to that of SOS^{HDPC} in a PIP_2-dependent manner.

is due to an overall destabilization of the inactive state, we compared the activity of SOS^{HDPC} to two SOS constructs containing PH domain-associated Noonan syndrome mutations, $SOS^{HDPC(E433K)}$, and $SOS^{HDPC(C441Y)}$, in the absence and presence of PIP_2 in Ras-coupled vesicles. In the absence of PIP_2, all of the SOS constructs ($SOS^{HDPC(E433K)}$, $SOS^{HDPC(C441Y)}$, and SOS^{HPDC}) show very low levels of activity, essentially indistinguishable from background (Fig. 6). However, inclusion of PIP_2 in membranes results in a marked increase in the activity of SOS constructs bearing the Noonan syndrome-associated mutations ($SOS^{HDPC(E433K)}$ and $SOS^{HDPC(C441Y)}$) (Fig. 6). The observation that the Noonan syndrome-associated mutations, $SOS^{HDPC(E433K)}$ and $SOS^{HDPC(C441Y)}$, are repressed in the absence of PIP_2 in membranes (Fig. 6) implies that the increase in SOS activity associated with these mutations is likely due to an uncoupling of the inhibitory conformations of the histone domain and the DH-PH unit, perhaps by altering the responsiveness of SOS to PIP_2. Additional studies will help to resolve this issue.

Concluding Remarks

We have shown previously that the N-terminal regulatory segment of SOS blocks the localization of SOS to the membrane by allosteric Ras, and that high membrane densities of PIP_2 and allosteric Ras synergize to release the inhibition of the DH-PH unit, opening the allosteric site. We have also shown that the histone domain constrains the activation of SOS by regulating the responsiveness of the PH domain to PIP_2, ensuring that full activation of SOS occurs only in the presence of input signals that are sufficiently strong to overcome the inhibition (9).

Here we present the crystal structure of autoinhibited SOS^{HDPC}. The structure reveals that the histone domain stabilizes the autoinhibited conformation of SOS by directly participating in the occlusion of the allosteric Ras binding site and by reinforcing the position of the PH-Rem linker and the inhibitory DH domain. In conjunction with the structural analysis, results from our in vitro activity assays of SOS and constructs of SOS containing mutations in the histone, DH, and PH domains indicate that the histone domain and the DH-PH unit are conformationally coupled, and that one component of the activation mechanism of SOS involves a membrane-dependent electrostatic switch in the configuration of the histone domain that coincides with increased accessibility of the allosteric site of SOS at the membrane. Thus, in addition to its important role in maintaining SOS in the autoinhibited conformation, the N-terminal regulatory segment seems to be crucial for effective membrane-binding and activation of SOS on membranes. In the active state, the histone domain might also play a role in regulating the membrane-residence of SOS, allowing SOS to act more efficiently at the membrane surface. This property, where the autoinhibitory domains take on a new role in the activated molecule, is not uncommon (28, 29).

Multiple domains in the same protein can cooperate with one another to drive membrane-binding (30). Our results support a model for three mechanisms that couple SOS to the membrane, in addition to recruitment to activated receptors by Grb2. First, a PH domain-PIP_2 binding interaction, second, nonspecific electrostatic interactions between the conserved positively charged region on the surface of the histone domain and the negatively charged membrane, and finally, the engagement of membrane-bound Ras at the allosteric site of SOS (Fig. 7). Other factors, such as the generation of PA by PLD2 (15, 27), are also likely to play a role. Our results suggest that the binding of the histone domain to the membrane is driven by electrostatic interactions. High levels of PA in membranes enhances the negative charge potential of the membrane surface in the local vicinity, and is therefore expected to increase the affinity of the histone domain for the membrane. Notably, high levels of PA should coincide with high levels of PIP_2, because the generation of PA is required for the activation of PI-4-P 5-kinase, which generates PIP_2. PIP_2 is a critical cofactor for PLD2, and a positive feedback loop between PLD2 and PI-4-P 5-kinase has been reported (31–33), possibly explaining the increased efficiency of membrane-binding and the consequent activation of SOS in response to

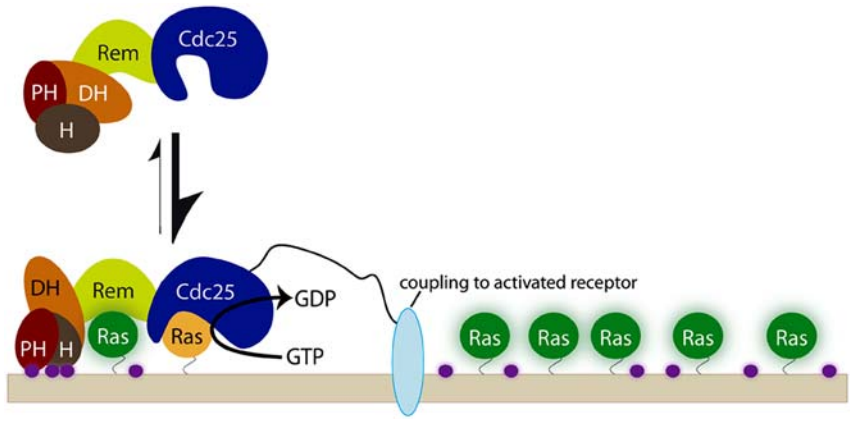

Fig. 7. Membrane-association of SOS is enhanced by cooperation of multiple membrane-binding interactions. Membrane-association of SOS is regulated by (*i*) the coupling to activated receptors, (*ii*) a PH domain-PIP_2 (purple circles) binding interaction, (*iii*) nonspecific electrostatic interactions between the membrane and a putative membrane-binding surface on the histone domain, and (*iv*) the engagement of Ras at the allosteric site. The synergistic combination of these membrane-binding events drives the release of autoinhibition and facilitates the productive reorientation of SOS in the plane of the membrane, maximizing the accessibility of both Ras binding sites of SOS at the membrane.

the generation of PA by PLD2. In the case of SOS, such a multi-layered mechanism of membrane-binding would facilitate the processive activation of Ras by SOS, allowing SOS to activate multiple Ras molecules before disengaging from the membrane.

Materials and Methods

Protein Preparation. SOS^{DPC} (residues 198–1049) and SOS^{HDPC} (residues 1–1049) of human SOS1 and $Ras^{(C118S)}$ (residues 1–181, C118S) of human H-Ras were expressed and purified as described (9, 19). Point mutations were introduced using the Quikchange site-directed mutagenesis kit (Stratagene) and confirmed by DNA sequencing.

Crystallization and Structure Determination. Crystals of SOS^{HDPC} (residues 1–1049) were grown at room temperature using hanging-drop vapor diffusion by mixing equal volumes of protein (20 mg/ml) and reservoir solutions [140–190 mM sodium thiocyanate, 14%–16% PEG 3350, 0.1 M SPG (succinic acid, phosphate, glycine) buffer (pH 6.0 or 6.5)[. Crystals were cryoprotected with the addition of 20% glycerol, and x-ray diffraction data were collected (Advanced Light Source, Beamline 8.2.2) on crystals flash frozen in liquid nitrogen.

Data were processed with HKL2000 (34) and the structure was solved by molecular replacement using Phaser (35) and the histone (18), DH (10), Rem and Cdc25 domains (8). Refinement and model building were performed with phenix.refine and Coot, respectively (36, 37). Figures were prepared using PyMOL.

Nucleotide Exchange Assays. Ras-coupled lipid vesicles were prepared as described (9). Nucleotide exchange reactions using Ras-coupled lipid vesicles were initiated by rapid mixing of 100 μl of 200 nM SOS with 100 μl of Ras-mant-dGDP-conjugated vesicles using a stopped flow apparatus (RX2000; Applied Photophysics) linked to a Fluoromax-3 fluorimeter (HORIBA Jobin Yvon). The surface density of Ras varied across experiments, but the total concentration of Ras stock before mixing was kept constant at 2 μM. Reaction progress was monitored by fluorescence intensity at 430 nm with 370 nm excitation. Reactions were performed at 25 °C in reaction buffer supplemented with 2 mM unlabeled GTP nucleotide. Data were obtained by repeating reactions on different days with different protein samples and different Ras-coupled vesicle preparations. The data were fit to a single-exponential decay function using the program Prism 4 (Graphpad Prism, Inc.).

ACKNOWLEDGMENTS. We thank T. Freedman, M. Lamers, R. McNally and J. Winger for helpful discussions and D. King for mass spectrometry. We also thank the staff at beamline 8.2.2 of the Advanced Light Source (Berkeley, CA).

1. Boriack-Sjodin PA, Margarit SM, Bar-Sagi D, Kuriyan J (1998) The structural basis of the activation of Ras by Sos. *Nature*, 394:337–343.
2. Schlessinger J (2000) Cell signaling by receptor tyrosine kinases. *Cell*, 103:211–225.
3. Margarit SM, et al. (2003) Structural evidence for feedback activation by Ras.GTP of the Ras-specific nucleotide exchange factor SOS. *Cell*, 112:685–695.
4. Freedman TS, et al. (2009) Differences in flexibility underlie functional differences in the Ras activators son of sevenless and Ras guanine nucleotide releasing factor 1. *Structure*, 17:41–53.
5. Das J, et al. (2009) Digital signaling and hysteresis characterize Ras activation in lymphoid cells. *Cell*, 136:337–351.
6. Roose JP, Mollenauer M, Ho M, Kurosaki T, Weiss A (2007) Unusual interplay of two types of Ras activators, RasGRP and SOS, establishes sensitive and robust Ras activation in lymphocytes. *Mol Cell Biol*, 27:2732–2745.
7. Boykevisch S, et al. (2006) Regulation of ras signaling dynamics by Sos-mediated positive feedback. *Curr Biol*, 16:2173–2179.
8. Sondermann H, et al. (2004) Structural analysis of autoinhibition in the Ras activator son of sevenless. *Cell*, 119:393–405.
9. Gureasko J, et al. (2008) Membrane-dependent signal integration by the Ras activator son of sevenless. *Nat Struct Mol Biol*, 15:452–461.
10. Soisson SM, Nimnual AS, Uy M, Bar-Sagi D, Kuriyan J (1998) Crystal structure of the Dbl and pleckstrin homology domains from the human son of sevenless protein. *Cell*, 95:259–268.
11. Zheng J, et al. (1997) The solution structure of the pleckstrin homology domain of human SOS1. A possible structural role for the sequential association of diffuse B cell lymphoma and pleckstrin homology domains. *J Biol Chem*, 272:30340–30344.
12. Koshiba S, et al. (1997) The solution structure of the pleckstrin homology domain of mouse son-of-sevenless 1 (mSos1). *J Mol Biol*, 269:579–591.
13. Kubiseski TJ, Chook YM, Parris WE, Rozakis-Adcock M, Pawson T (1997) High affinity binding of the pleckstrin homology domain of mSos1 to phosphatidylinositol (4,5)-bisphosphate. *J Biol Chem*, 272:1799–1804.
14. Chen RH, Corbalan-Garcia S, Bar-Sagi D (1997) The role of the PH domain in the signal-dependent membrane targeting of Sos. *Embo J*, 16:1351–1359.
15. Zhao C, Du G, Skowronek K, Frohman MA, Bar-Sagi D (2007) Phospholipase D2-generated phosphatidic acid couples EGFR stimulation to Ras activation by Sos. *Nat Cell Biol*, 9:706–712.
16. Sullivan SA, Aravind L, Makalowska I, Baxevanis AD, Landsman D (2000) The histone database: A comprehensive WWW resource for histones and histone fold-containing proteins. *Nucleic Acids Res*, 28:320–322.
17. Baxevanis AD, Arents G, Moudrianakis EN, Landsman D (1995) A variety of DNA-binding and multimeric proteins contain the histone fold motif. *Nucleic Acids Res*, 23:2685–2691.
18. Sondermann H, Soisson SM, Bar-Sagi D, Kuriyan J (2003) Tandem histone folds in the structure of the N-terminal segment of the Ras activator son of sevenless. *Structure*, 11:1583–1593.
19. Sondermann H, Nagar B, Bar-Sagi D, Kuriyan J (2005) Computational docking and solution x-ray scattering predict a membrane-interacting role for the histone domain of the Ras activator son of sevenless. *Proc Natl Acad Sci USA*, 102:16632–16637.
20. Tartaglia M, Gelb BD (2005) Noonan syndrome and related disorders: Genetics and pathogenesis. *Annu Rev Genom Hum G*, 6:45–68.
21. Roberts AE, et al. (2007) Germline gain-of-function mutations in SOS1 cause Noonan syndrome. *Nat Genet*, 39:70–74.
22. Tartaglia M, et al. (2007) Gain-of-function SOS1 mutations cause a distinctive form of Noonan syndrome. *Nat Genet*, 39:75–79.
23. Buday L, Downward J (1993) Epidermal growth factor regulates p21ras through the formation of a complex of receptor, Grb2 adapter protein, and Sos nucleotide exchange factor. *Cell*, 73:611–620.
24. Egan SE, et al. (1993) Association of Sos Ras exchange protein with Grb2 is implicated in tyrosine kinase signal transduction and transformation. *Nature*, 363:45–51.
25. Li N, et al. (1993) Guanine-nucleotide-releasing factor hSos1 binds to Grb2 and links receptor tyrosine kinases to Ras signalling. *Nature*, 363:85–88.
26. Gale NW, Kaplan S, Lowenstein EJ, Schlessinger J, Bar-Sagi D (1993) Grb2 mediates the EGF-dependent activation of guanine nucleotide exchange on Ras. *Nature*, 363:88–92.
27. Yadav KK, Bar-Sagi D (2010) Allosteric Gating of Sos Activity by the Histone Folds Domain. *Proc Natl Acad Sci USA*, XXX pp:XXX–XXX.
28. Kim AS, Kakalis LT, Abdul-Manan N, Liu GA, Rosen MK (2000) Autoinhibition and activation mechanisms of the Wiskott–Aldrich syndrome protein. *Nature*, 404:151–158.
29. Cai X, et al. (2008) Spatial and temporal regulation of focal adhesion kinase activity in living cells. *Mol Cell Biol*, 28:201–214.
30. Lemmon MA (2008) Membrane recognition by phospholipid-binding domains. *Nat Rev Mol Cell Biol*, 9:99–111.
31. Sciorra VA, et al. (2002) Dual role for phosphoinositides in regulation of yeast and mammalian phospholipase D enzymes. *J Cell Biol*, 159:1039–1049.
32. Jenkins GH, Fisette PL, Anderson RA (1994) Type I phosphatidylinositol 4-phosphate 5-kinase isoforms are specifically stimulated by phosphatidic acid. *J Biol Chem*, 269:11547–11554.
33. Foster DA, Xu L (2003) Phospholipase D in cell proliferation and cancer. *Mol Cancer Res*, 1:789–800.
34. Otwinowski Z, Minor W (1997) Processing of X-ray diffraction data collected in oscillation mode. *Method Enzymol*, 276:307–326.
35. McCoy AJ, Grosse-Kunstleve RW, Storoni LC, Read RJ (2005) Likelihood-enhanced fast translation functions. *Acta Crystallogr D*, 61:458–464.
36. Emsley P, Cowtan K (2004) Coot: Model-building tools for molecular graphics. *Acta Crystallogr D* , 60:2126–2132.
37. Adams PD, et al. (2002) PHENIX: Building new software for automated crystallographic structure determination. *Acta Crystallogr D*, 58:1948–1954.
38. Baker NA, Sept D, Joseph S, Holst MJ, McCammon JA (2001) Electrostatics of nanosystems: Application to microtubules and the ribosome. *Proc Natl Acad Sci USA*, 98:10037–10041.

Supporting Information

Gureasko et al. 10.1073/pnas.0913915107

SI Text

Fig. S1. Alignment of SOS sequences from human (SOS1_human and SOS2_human), mouse (SOS1_mouse), mosquito (SOS_*a nopheles*), fruit fly (SOS_*DROME*), and worm (*Caenorhabditis*). The alignment was generated using ClustalW (1). Increasing levels of blue correspond to increasing homology above 30% conservation. Boxes designate invariant and highly conserved residues located in the interface between the histone domain, the DH domain and the PH-Rem linker. Accession numbers are as follows: human SOS1, Q07889; mouse SOS1, Q62245; human SOS2, Q07890; *Drosophila melanogaster* SOS, P26675; *Anopheles gambiae* SOS, XP_319944; *Caenorhabditis elegans* SOS, NP_504235.

1. Thompson JD, Higgins DG, & Gibson TJ (1994) CLUSTAL W: Improving the sensitivity of progressive multiple sequence alignment through sequence weighting, position-specific gap penalties and weight matrix choice. *Nucleic Acids Res* 22:4673–4680.

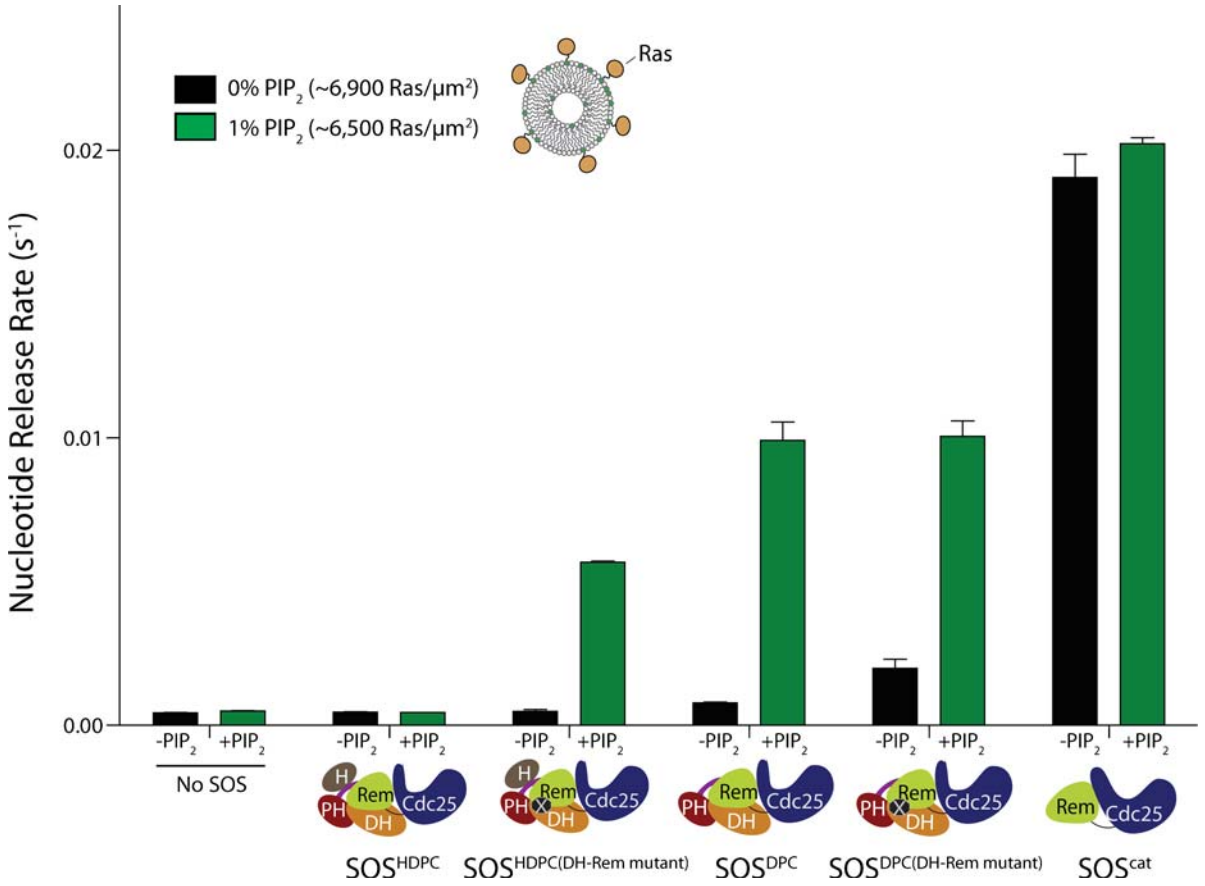

Fig. S2. The PH domain-PIP_2 binding interaction is required for full relief of inhibition by the DH domain. Nucleotide exchange rates for SOS^{HDPC}, $SOS^{HDPC(DH\text{-}Rem\ interface\ mutant)}$, SOS^{DPC}, $SOS^{DPC(DH\text{-}Rem\ interface\ mutant)}$ and SOS^{cat} are compared in the absence and presence of PIP_2 in Ras-coupled vesicles. In these reactions, mant-dGDP is exchanged for unlabeled GTP (bulk concentration of Ras and SOS is 1 μM and 10 nM, respectively). $SOS^{HDPC(DH\text{-}Rem\ interface\ mutant)}$ and $SOS^{DPC(DH\text{-}Rem\ interface\ mutant)}$ are mutant forms of SOS^{HDPC} and SOS^{DPC} that contain mutations (E268A, M269A and D271A) that weaken the DH-Rem interface (1). Note that inclusion of 1% PIP_2 in Ras-coupled vesicles results in a substantial increase in the activity of $SOS^{HDPC(DH\text{-}Rem\ interface\ mutant)}$, $SOS^{DPC(DH\text{-}Rem\ interface\ mutant)}$ and SOS^{DPC}.

1. Sondermann H et al. (2004) Structural analysis of autoinhibition in the Ras activator son of sevenless. *Cell* 119:393–405.

Table S1. Data Collection and Refinement Statistics

Space group	$C222_1$
Unit cell	a = 150.96 Å b = 160.92 Å c = 118.87 Å
X-ray source	ALS 8.2.2
Wavelength (Å)	1.000
Resolution range (Å)	50.00 – 3.18 (3.31 – 3.18)[a]
Measured reflections	538,686
Unique reflections	24,554
Number of protein atoms	8210
R_{sym}[b] (%)	9.6 (81.6)
R_{work}[c]/R_{free}[d] (%)	26.0/31.2
Redundancy (%)	7.7 (6.5)
I/σ[e]	22.8 (2.25)
Completeness (%)	99.9 (99.3)
Rmsd bond length (Å)	0.002
Rmsd angles (°)	0.527

[a]Values in parentheses refer to the highest resolution shell.
[b]$R_{sym} = 100 \times \Sigma|I - \langle I\rangle|/\Sigma I$, where I is the integrated intensity of a measured reflection.
[c]$R_{work} = \Sigma|F_{obs} - \langle F_{calc}\rangle|/\Sigma\ F_{obs}$
[d]R_{free} is R_{work} for 8% of reflections selected at random and omitted from refinement.
[e]I/σ equals mean signal to noise.